Polymer 50 (2009) 107–116

Contents lists available at ScienceDirect

Polymer

journal homepage: www.elsevier.com/locate/polymer

Preparation and evaluation of thermo-reversible copolymer hydrogels containing chitosan and hyaluronic acid as injectable cell carriers

Jyh-Ping Chen*, Tai-Hong Cheng

Department of Chemical and Materials Engineering, Chang Gung University, Kwei-San, Taoyuan 333, Taiwan, ROC

ARTICLE INFO

Article history:
Received 18 September 2008
Received in revised form
22 October 2008
Accepted 24 October 2008
Available online 5 November 2008

Keywords:
Hydrogel
Poly(*N*-isopropylacrylamide)
Chitosan

ABSTRACT

Poly(*N*-isopropylacrylamide) end-capped with a carboxyl group (PNIPAM-COOH) was grafted to chitosan for synthesizing thermo-reversible chitosan-*g*-poly(*N*-isopropylacrylamide) (CPN), which was further grafted with hyaluronic acid (HA) to form hyaluronic acid-*g*-CPN (HA–CPN). PNIPAM-COOH, CPN and HA–CPN formed injectable free-flowing aqueous solutions and exhibited reversible sol-to-gel phase transition (above 5% polymer concentration) at 30 °C. Chemical properties and temperature-dependent physical properties of the polymer hydrogels, such as rheological behavior, phase transition kinetics, and water content were characterized in detail. The mechanical stiffness of hydrogels increased with the presence of chitosan in the copolymer, but decreased after conjugation with HA. Chitosan and HA grafting also endowed higher water content and resistance to volume contraction during phase change of the copolymer solution. *In vitro* cell culture experiments with chondrocytes and meniscus cells in HA–CPN hydrogel showed beneficial effects on the cell phenotypic morphology, proliferation, and differentiation. Progressive tissue formation was demonstrated by monotonic increases in extracellular matrix contents and mechanical properties.

1. Introduction

Many studies have evaluated the potential of using polymeric biomaterials as three-dimensional (3D) scaffolds for articular cartilage and meniscus, and demonstrated that cellular functions exhibited in monolayer culture are quite different from those obtained from 3D culture systems [1]. To successfully achieve articular cartilage and meniscus tissue regeneration, the scaffold should contain interconnected pores and provide adequate mechanical strength, and closely mimic the *in vivo* environment of the knee joint by consisting of components of the cartilage- and meniscus-specific extracelluar matrix (ECM), such as type I and II collagens, chondroitin sulfate, and hyaluronic acid [2].

Chitosan, derived from chitin by deacetylation, is a linear polysaccharide consisting of β-(1,4) linked D-glucosamine residues and *N*-acetyl-glucosamine groups [3]. Chitosan has been widely used in biomedical applications due to its biocompatibility, nontoxicity, bioactivity, biodegradability, and ease of modification through hydroxyl and amine groups [4]. Moreover, the structure of chitosan is very similar to glycosaminoglycans (GAGs) discovered in cartilage and meniscus so that it can mimic the *in vivo* environment for cultivating chondrocytes and meniscus cells [5]. Hyaluronic acid (HA) is a natural polysaccharide consisting of alternate *N*-acetyl-D-glucosamine and D-glucuronic acid linked by (1 → 3) and (1 → 4) glycoside bonds. HA is a key component of ECM in connective tissues and is particularly abundant in the synovial fluid with its high water adsorption and retention capability [6]. This highly viscous and viscoelastic fluid is found in joint cavities, and serves as a lubricant and shock absorber for the protection of joints and bones [7]. HA is known to influence chondrocytes by triggering a sophisticated signaling pathway leading to enhancement of cellular functions [8].

Intelligent biopolymer systems with *in situ* gel-forming capability have recently been of increasing importance in the development of therapeutic implants and drug delivery systems [9,10]. Poly(*N*-isopropylacrylamide) (PNIPAM) is a well-known thermo-responsive polymer exhibiting reversible sol-to-gel phase transition behavior in water. It is soluble in water when temperature is below its lower critical temperature (LCST) around 30 °C and precipitates out of the solution above this temperature [11]. PNIPAM can be modified with chitosan, collagen, HA, gelatin or other natural polymers to adjust the gelling temperature to be close to physiological conditions, to strengthen its mechanical strength, and to make the hydrogel more biocompatible [12–18]. Taking advantage of the sol–gel phase transition of PNIPAM-based copolymer,

* Corresponding author. Tel.: +886 3 2118800; fax: +886 3 2118668.
E-mail address: jpchen@mail.cgu.edu.tw (J.-P. Chen).

0032-3861/$ – see front matter © 2008 Elsevier Ltd. All rights reserved.
doi:10.1016/j.polymer.2008.10.045

cells could be uniformly mixed with the copolymer in culture medium and quickly injected into a desirable tissue-damaged cavity area with a syringe by operating at temperatures below LCST [19]. The polymer solution will be gelled *in situ* after injection at physiological temperature and the rigid hydrogel could provide 3D structure suitable for cell proliferation, migration, and ECM secretion [20]. Injectable hydrogel as cell carrier may be more suitable for treating irregularly shaped defects than rigid scaffolds, with the procedure being simpler, more time-saving and cost-effective than open surgery [21].

Previously, we reported the synthesis of chitosan-*g*-poly(*N*-isopropylacrylamide) (CPN), a thermo-responsive comb-like polymer with chitosan as the backbone and pendant PNIPAM groups, by grafting PNIPAM-COOH with a single carboxyl end group onto chitosan through amide bond linkages [22,23]. *In vitro* cell culture experiments demonstrated usefulness of this hydrogel as an injectable cell carrier [22]. In this study, to further improve properties of the injectable scaffold, HA was grafted to CPN to form hyaluronic acid-*g*-CPN (HA–CPN) [24,25]. Hydrogels containing PNIPAM-COOH, CPN, and HA–CPN were fully characterized and compared in addition to evaluate their potentials as injectable 3D cell carriers for chondrocytes and meniscus cells.

2. Experimental section

2.1. Materials

N-isopropylacrylamide (NIPAM, Aldrich) and azobisisobutyronitrile (AIBN, Sigma) were recrystallized from *n*-hexane and methanol, respectively, freshly before use. Mercaptoacetic acid (MAA, Fluka) was utilized as a chain transfer agent to obtain PNIPAM-COOH. Chitosan (degree of deacetylation = 98%, molecular weight = 1.5×10^5) was obtained from Fluka. 1-Ethyl-3-(3-dimethylaminopropyl) carbodiimide (EDC) and *N*-hydroxysuccinimide (NHS) were obtained from Acros. 2-Morpholinoethane sulfonic acid (MES) and 2,4,6-trinitrobenzene sulfonic acid (TNBS) were purchased from Sigma. HA was obtained from fermentation of *Streptococcus zooepidemicus* with weight average molecular weight = 1.78×10^6 Da, polydispersity = 1.68 from size exclusion chromatography [26]. Dulbecco's modified Eagle's medium F-12 Han (F-12 DMEM, Sigma) and fetal bovine serum (HyClone) were used for culture primary rabbit articular chondrocytes and meniscus cells.

2.2. Synthesis of PNIPAM-COOH, CPN, and HA–CPN polymers

PNIPAM-COOH with a carboxylic acid-ended group was prepared in benzene by free radical polymerization (Scheme 1) between NIPAM monomers and MAA by using AIBN as an initiator [22]. To synthesize CPN copolymer, 0.5 g chitosan and 5 g PNIPAM-COOH were dissolved in 50 ml MES buffer (0.1 M, pH 5) containing EDC and NHS. After reacting at 25 °C, 180 rpm for 12 h, the copolymer was purified by thermally induced precipitation [22]. For HA–CPN synthesis, a mixture of CPN and HA (0.25 g) was dissolved in 100 ml of 0.1 M MES buffer (pH 5) and the grafting reaction was carried out at 25 °C, 180 rpm for 12 h in the presence of 0.46 g EDC and 1.37 g NHS. After the reaction, impurities and residual HA were simultaneously removed by precipitation at 50 °C. Purified HA–CPN copolymer could be obtained after dialysis (MWCO 300,000) at 4 °C for 4 d and lyophilization.

2.3. Molecular weight of copolymer hydrogels

The average molecular weight of PNIPAM-COOH was determined by end-group titration where 0.5 g polymer dissolved in 10 ml water was titrated with 0.01 N NaOH. For CPN and HA–CPN, the grafting ratio (GR) was calculated based on weight change with the following equations.

$$\text{Grafting ratio of CPN} = \frac{(W_{\text{CPN}} - W_{\text{C}})/\text{MW}_{\text{PNIPAM}}}{W_{\text{C}}/\text{MW}_{\text{C}}} \quad (1)$$

$$\text{Grafting ratio of HA—CPN} = \frac{W_{\text{CPN}}/\text{MW}_{\text{CPN}}}{(W_{\text{HA—CPN}} - W_{\text{CPN}})/\text{MW}_{\text{HA}}} \quad (2)$$

where W_{CPN}, W_{C}, and $W_{\text{HA–CPN}}$ denote the weight of CPN, chitosan and HA–CPN, respectively; MW_{C}, $\text{MW}_{\text{PNIPAM}}$ and MW_{HA} denote the molecular weight of chitosan, PNIPAM-COOH and HA, respectively. The molecular weight of CPN (MW_{CPN}) and HA–CPN ($\text{MW}_{\text{HA–CPN}}$) could be determined with the following equations.

$$\text{MW}_{\text{CPN}} = \text{MW}_{\text{C}} + \text{MW}_{\text{PNIPAM}} \times \text{GR for CPN} \quad (3)$$

$$\text{MW}_{\text{HA—CPN}} = \text{MW}_{\text{HA}} + \text{MW}_{\text{CPN}} \times \text{GR for CPN—HA} \quad (4)$$

2.4. Determination of amino groups in copolymers

The number of amino groups in CPN and HA–CPN, which were on chitosan backbone, was determined by TNBS method. Primary amines, upon reaction with TNBS, form a highly chromogenic derivative, which can be measured at 335 nm. Quantitative determination of the number of free amino groups available within a sample was accomplished in comparison with a standard curve generated using glucosamine. The percentage of amino group reacted in each polymer sample was calculated by considering the weight of polymer used in the reaction.

2.5. Lower critical solution temperature (LCST)

Polymer solutions were prepared in DDI water at concentrations of 5 and 10% (w/v). The phase transition of polymer solutions was measured using an UV/VIS spectrophotometer (Thermo Spectronic) equipped with a circulator bath for temperature control. The absorbance of visible light ($\lambda = 470$ nm; path length = 1 cm) through the polymer solution was recorded at increasing temperature from 25 to 33 °C at a rate of 1/3.5 °C/min, followed by decreasing temperature from 33 to 25 °C at a rate of 1/6.0 °C/min. At each test temperature, polymer solution was equilibrated for 3 min to reach thermodynamic equilibrium. Once the thermo-precipitation and dissolution curves were obtained by plotting absorbance vs. temperature, the LCST of polymer solution was defined as the temperature where solution turbidity is half of the maximum value.

2.6. Phase transition kinetics

Different concentrations (5 and 10% (w/v)) of polymer aqueous solutions were prepared in a cuvette and sealed with Parafilm. For gel forming kinetics, the samples were equilibrated in a 25 °C incubator for 1 h, and then placed in an UV–vis spectrophotometer pre-equilibrated at 37 °C. The turbidity of polymer solution was recorded as a function of time. For gel liquefaction kinetics, a similar procedure was followed by changing the temperature from 37 to 25 °C. The gel formation (or liquefaction) time was defined as the time at which the absorbance reached half of the maximum (minimum) value.

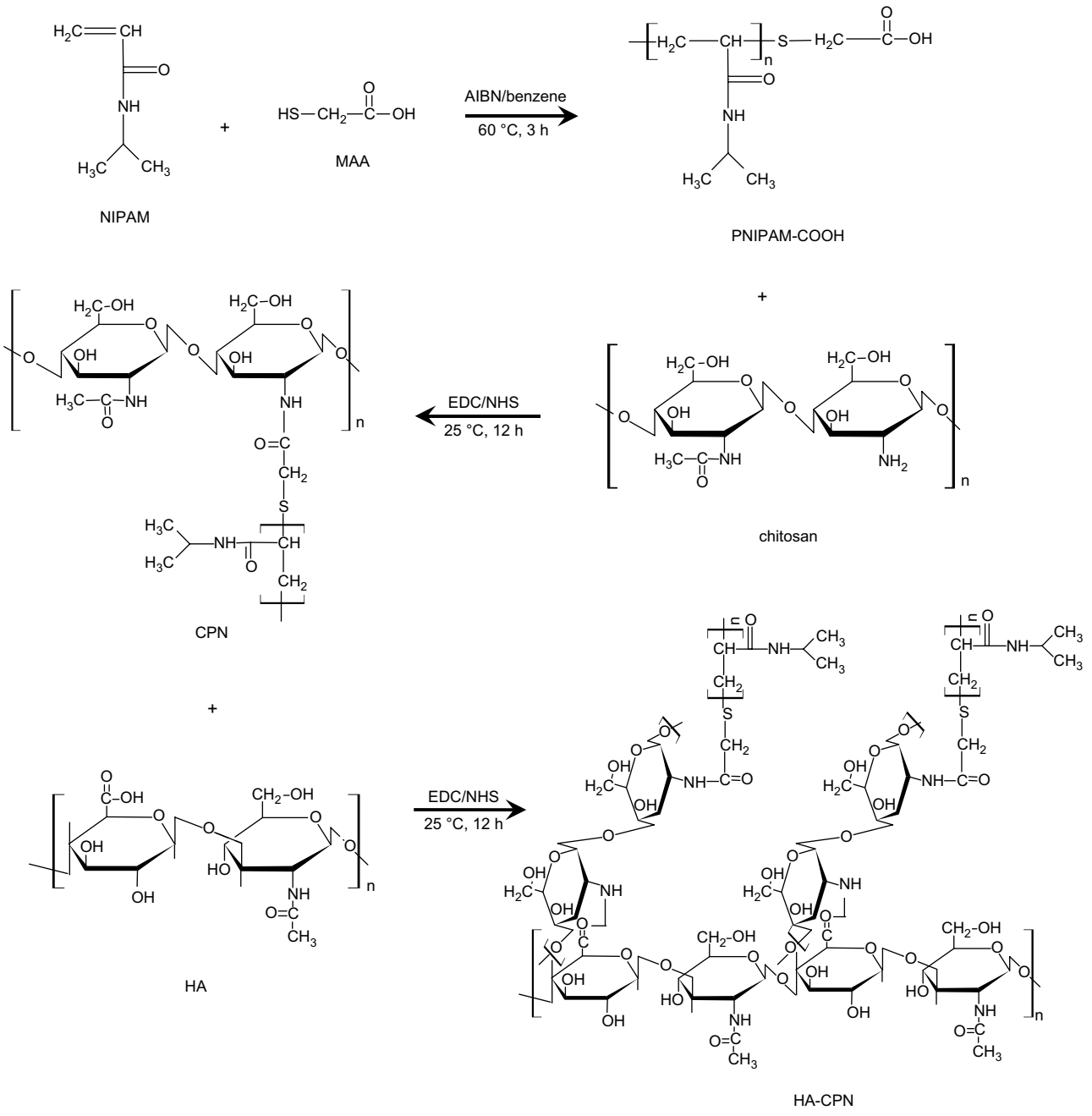

Scheme 1. Synthesis route of PNIPAM-COOH, chitosan-*g*-PANIPAM (CPN), and hyaluronic acid-*g*-CPN (HA–CPN).

2.7. Water content and volume shrinkage

To examine water content of hydrogels, 1 ml of polymer aqueous solution (5, 10, and 20% (w/v)) was placed in a 37 °C incubator for 1 h. After gelation, extra 1 ml DDI water was added to ensure hydrogel wettability. After incubation at 37 °C for another 2 d, the supernatant was discarded and the wet hydrogel was weighed. The water content of polymer hydrogels was determined from the weight difference of hydrogels before and after phase transition.

$$\text{Water content} = \frac{W_{\text{hydrogel}} - W_{\text{polymer}}}{W_{\text{polymer}}} \tag{5}$$

where W_{polymer} is the dry weight of the polymer, and W_{hydrogel} is the weight of hydrogel after gelation at 37 °C.

The volume shrinkage (%) of polymer hydrogel was defined as the percentage of water volume loss after polymer solutions gelled at 37 °C.

$$\begin{aligned}\text{Volume shrinkage}\ (\%) &= -\left(1 - \frac{V_{\text{i}} - V_{\text{H}_2\text{O}}}{V_{\text{i}}}\right) \times 100\% \\ &= -\left(1 - \frac{V_{\text{w}}}{V_{\text{i}}}\right) \times 100\% \\ &= -\frac{V_{\text{H}_2\text{O}}}{V_{\text{i}}} \times 100\% \end{aligned} \tag{6}$$

where V_{i} is the volume of initial polymer solution at 25 °C, $V_{\text{H}_2\text{O}}$ is the volume of water squeezed out as polymer hydrogel formed, and V_{w} is the volume of water in polymer hydrogel after gelation.

2.8. Physical and rheological properties

To understand the rheological behavior, oscillatory analysis of all hydrogel samples was performed using a Carri-Med CSL^2 100 controlled stress rheometer (TA Instruments) as a function of temperature and frequency. The storage modulus (G'), loss modulus (G''), and apparent dynamic viscosity (η_a) were determined using Rheology Solutions software provided by TA Instruments. G' gives information about the elasticity or the energy stored in the material during deformation, whereas G'' describes the viscous character or the energy dissipated as heat. The combined viscous and elastic behavior is given by the absolute value of complex shear modulus $G^* = \sqrt{G'^2 + G''^2}$. The modulus and viscosity data were recorded by continuously increasing temperature at a rate of 3 °C/min. Other parameter settings are described as the following: 60 mm cone-plate, gap = 52 μm, shear stress = 2 Pa, and 10 min ramp duration for viscosity experiments; 40 mm flat-plate, gap = 52 μm, shear stress = 1 Pa, and frequency = 0.5 Hz for modulus measurements as a function of temperature. The viscoelastic properties of the gelled samples as a function of frequency was determined at 37 °C by small-amplitude oscillatory shear experiments with 40 mm flat-plate and with gap = 52 mm, shear strain = 20%, frequency = 0.01–10 Hz.

The frequency-dependence of the dynamic viscosity was fitted to the modified Cross-equation to compare the shear thinning properties of different hydrogels [27].

$$\eta_a = \eta_\infty + \left(\frac{\eta_0 - \eta_\infty}{1 + (kF)^n}\right) \quad (7)$$

where η_a is the apparent dynamic viscosity, η_0 and η_∞ are limiting viscosities at zero and infinite shear rate, F is shear rate, k is a fitting parameter, and n is the slope of the frequency-dependent region that can be considered as a "pseudoplasticity index".

Wide angle X-ray diffraction (WAXD) spectra were registered with a Simens D5005 diffractometer composed of a CuK source, a quartz monochromator, and a goniometric plate at a scanning speed of 2° min^{-1} over the 2θ range from 5° to 30°. Surface potential was measured for different 1% (w/v) polymers in DDI water at room temperature using Zetasizer from Malvern. Thermogravimetric analysis (TGA) was conducted with TGA 2050 from TA Instruments.

2.9. Cell culture

Articular chondrocytes and meniscus were harvested from the knee articular cartilage and meniscus of a New Zealand rabbit [22,24]. After subculture for one passage, chondrocytes and meniscus cells were trypsinized and mixed with F-12 DMEM medium. For 3D hydrogel culture, 0.1 ml of cell solution was mixed with 0.5 ml of 10% (w/v) sterilized polymer solution at temperature below 25 °C, and then cultured in a 24-well plate (Nunc). After incubation in a 37 °C CO_2 incubator, polymer solutions became solid-like hydrogels and provided a porously 3D structure for cell cultivation. Two milliliter of culture medium was then added to each well and cell culture was carried out at 37 °C in a CO_2 incubator with medium change every two days. CellTiter 96® AQueous One Solution Cell Proliferation Assay Kits (methyl tetrazolium salt, MTS) (Promega) were used to determine cell proliferation as described previously [22]. Cell monolayer culture on tissue culture polystyrene (TCPS) was used as a control in all cases.

2.10. Cell assay and analysis

To determine GAG synthesis, cell pellets together with the hydrogel scaffolds were lyophilized and digested enzymatically with 1 ml of papain solution at 60 °C by shaking at 100 rpm for 24 h. The papain solution contained papain (50 μg/ml), sodium citrate (55 mM), sodium chloride (150 mM), cysteine·HCl (5 mM) and EDTA (5 mM). After digestion, the GAG content was determined quantitatively by 1,9-dimethylmethylene blue (Aldrich) with shark chondroitin sulfate C (Sigma) as a standard. The absorbance was measured at 525 nm by a UV/VIS spectrophotometer.

The total collagen secreted by chondrocytes and meniscus cells was assayed indirectly by measuring the hydroxyproline content using a colorimetric method. After hydrolyzation by papain, the absorbance of each sample was read at 540 nm using an ELISA reader after reaction with 4-dimethylamino-benzaldehyde (Riedel-deHaën). Total collagen content of the sample was estimated by assuming a hydroxyproline/collagen weight ratio of 0.125.

For scanning electron microscopy (SEM) observation, cell-containing hydrogel samples were fixed in glutaraldehyde, dehydrated in stepwise increasing concentrations of ethanol, dried in a critical point dryer, and examined by SEM (JEOL, ISM 5410) [22].

3. Results and discussion

3.1. Synthesis of CPN and HA–CPN copolymers

Several research articles have been reported on the graft copolymerization of PNIPAM onto other polymer backbones [12–18]. Our present report aims at the synthesis of CPN and HA–CPN copolymers based on the combination of PNIPAM-COOH, chitosan and HA in the presence of water-soluble EDC/NHS. CPN is a comb-like copolymer with PNIPAM side chain extending from the chitosan backbone [22,23]. The double grafted HA–CPN was synthesized by grafting CPN onto the HA molecules [24,25]. The results and properties of the synthesized polymers are summarized in Table 1.

The average molecular weight of PNIPAAM-COOH is 2.1×10^4 g/mol by end-group titration. The molar ratio of PNIPAM-COOH to chitosan during CPN synthesis will determine the number of PNIPAM chains grafted on a chitosan backbone, and subsequently influence the molecular weight of CPN. By controlling a low ratio of PNIPAM-COOH to chitosan during the grafting reaction, CPN with GR of 46 could be obtained and the molecular weight is 1.12×10^6 g/mol. Although CPN with high GR can be obtained, we chose to use CPN with low GR for synthesizing HA–CPN for its abundant amino groups for subsequent HA conjugation and high mechanical strength. HA–CPN was synthesized with 27 CPN chains grafted on a HA molecule, which gave HA–CPN with a molecular weight of 3.22×10^7 g/mol.

PNIPAM-COOH gives negative surface potential (−3.26 mV) due to the dissociation of its carboxyl end group in water. This surface potential becomes positive (8.64 mV) for CPN with the consumption of the –COOH groups and subsequent formation of the neutral

Table 1
Results and properties of synthesized PNIPAM-COOH, CPN and HA–CPN polymers.

Polymers	Grafting ratio[a]	Molecular weight[b] (g/mol)	Yield (%)	Surface potential[c](mV)
PNIPAM-COOH	–	2.10×10^4	73	-3.26 ± 0.39
CPN	46	1.12×10^6	67	8.64 ± 0.56
HA–CPN	27	3.22×10^7	94	-9.35 ± 1.17

[a] Grafting ratio for CPN is the number of PNIPAM-COOH chains grafted onto a chitosan molecule. Grafting ratio for HA–CPN is the number of CPN chains grafted onto a HA molecule.

[b] Molecular weight of PNIPAM-COOH was calculated from end-group titration. Molecular weight for CPN and HA–CPN was calculated from grafting ratio.

[c] The surface potential values of pure HA and chitosan were -47.8 ± 1.7 mV and 11.3 ± 0.3 mV, respectively. All experiments were conducted at room temperature with 1% (w/v) polymers in DDI water. Data were reported as mean ± standard deviation ($N = 5$).

amide groups, and the positive charge associated with the remaining amino groups in chitosan backbone. By grafting HA to CPN, the surface potential becomes highly negative again (−9.35 mV) owing to the introduction of excess carboxyl groups in HA (Table 1).

The synthesis of CPN and HA–CPN hydrogels could be followed by quantitative analysis of the amount of free amino groups on the chitosan moiety of the copolymers. For CPN, the percentage of free amino groups in chitosan reacted after PNIPAM-COOH conjugation was 7.9 ± 1.3%. However, after further grafting with HA this value increased sharply to 66.4 ± 1.1% due to the availability of abundant carboxyl groups in HA (one per subunit), which could react with the remaining amino groups in CPN. Taken together, the conjugation of PNIPAM-COOH to chitosan and CPN to HA through amide bond linkage could be confirmed.

As can be seen from TGA analysis in Fig. 1, the onsets of weight loss are 270, 310, and 400 °C for HA, chitosan, and PNIPAM-COOH, respectively. For PNIPAM-COOH, the weight loss reaches 100% at 430 °C and the peak temperature for the highest rate of weight loss temperature is 420 °C. This can be compared with chitosan and HA whose peak temperatures are 330 and 290 °C, respectively. The onset of weight loss of CPN is similar to PNIPAM-COOH (400 °C) but with 10 °C increase of the peak temperature (430 °C). By grafting HA to CPN, the onset of decomposition of HA–CPN is shifted back to that of HA at 270 °C and the highest decomposition rate occurred at 420 °C (similar to PNIPAM-COOH).

3.2. Properties of thermo-reversible polymers

Fig. 2 shows the temperature-dependent absorbance changes of different polymer solutions at 5 and 10% (w/v). During the heating cycle, a change in solution temperature from 25 to 33 °C resulted in dramatic increase of absorbance due to temperature-driven sol-to-gel transition. The subsequent cooling cycle resulted in gel-to-sol transition and fully reversible gel melting. The observed hysteresis loop, typical for polymeric networks, is a kinetically controlled phenomenon reflecting the resistance to disintegration of entangled polymer chains forming the hydrogel network. The LCST was not significantly affected by polymer concentration. At 10% (w/v) polymer concentration, HA–CPN had a slightly higher sol-to-gel phase transition temperature (*ca.* 30.3 °C) during the heating cycle in comparison to PNIPAM-COOH and CPN polymers (*ca.* 29.7 °C). Similarly, during the subsequent cooling cycle, HA–CPN showed lower gel-to-sol phase transition temperature (*ca.* 27.8 °C) than the other polymers (*ca.* 28.4 °C). Similar behavior was also observed at 5% (w/v) polymer concentration. The addition of HA to CPN increased LCST during gel forming and decreased LCST during gel melting due to its hydrophilic moieties such as carboxylic acid (–COOH) and hydroxyl (–OH) groups [28].

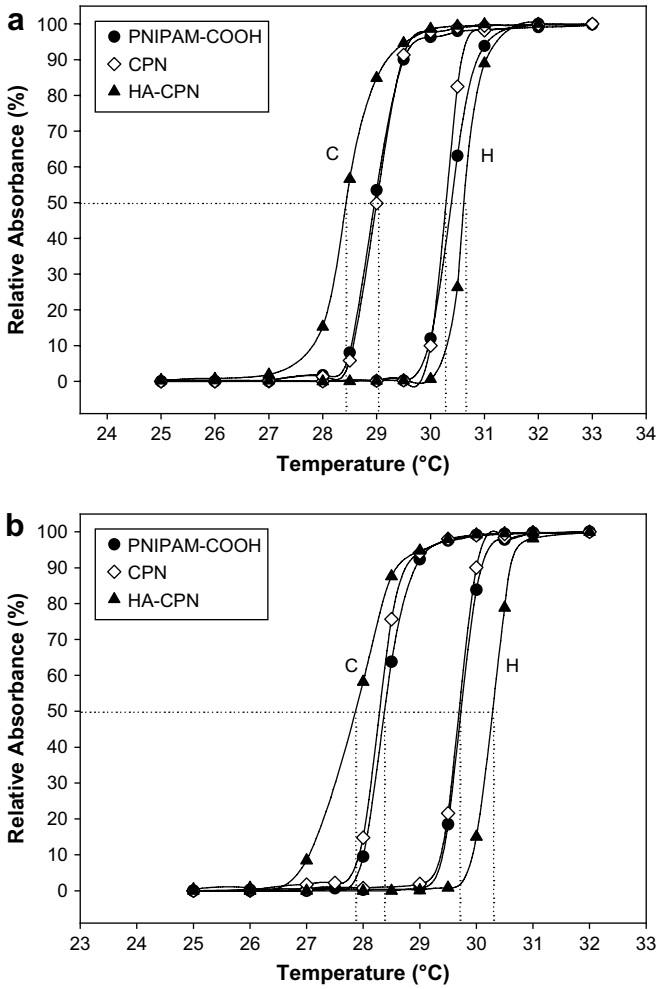

Fig. 2. Phase transition behavior of thermo-sensitive polymers at (a) 5% (w/v) and, (b) 10% (w/v). H indicates heating cycle from 25 to 33 °C whereas C indicates cooling cycle from 33 to 25 °C.

Phase transition kinetics analysis was carried out to investigate the gel formation time (GFT) of polymer solutions and the gel

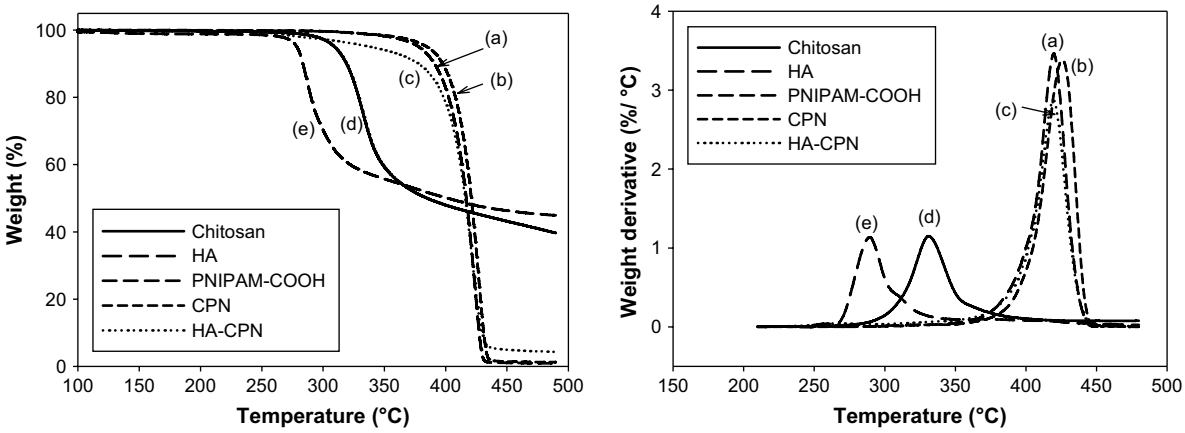

Fig. 1. Thermogravimetric (TGA) analysis of (a) PNIPAM-COOH, (b) CPN, (c) HA–CPN, (d) chitosan, (e) HA.

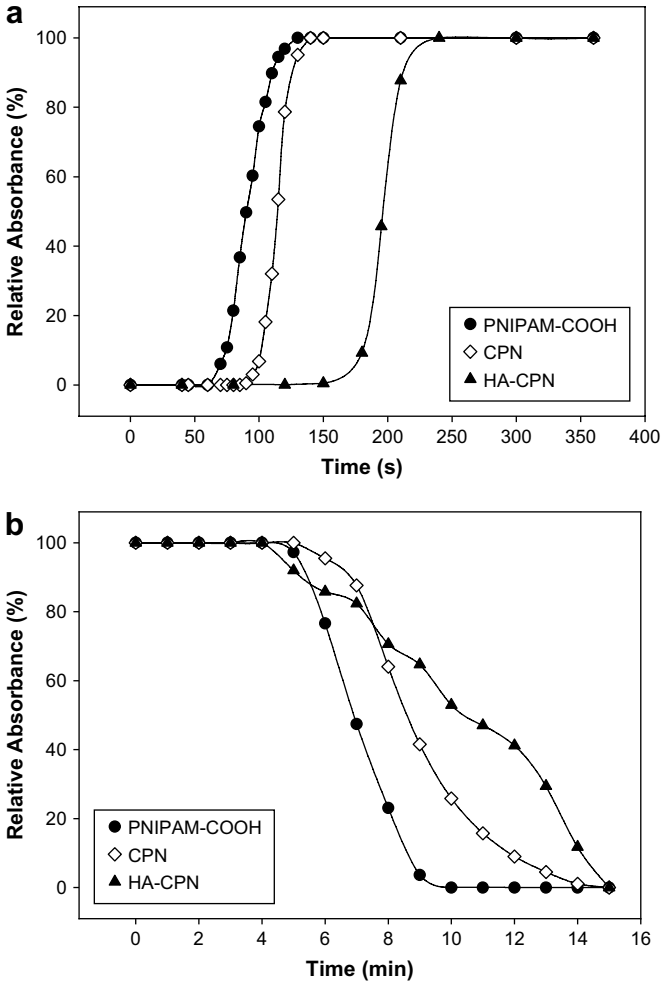

Fig. 3. Kinetics of phase transition of 10% (w/v) polymer solutions during (a) heating, and (b) cooling. The instantaneous temperature change is from 25 to 37 °C for heating and 37–25 °C for cooling.

liquefaction time (GLT) of polymer hydrogels. As shown in Fig. 3a, the relative absorbance rose sharply as surrounding temperature was shifted from 25 to 37 °C. The gel formation kinetics of CPN is slower than that of PNIPAM-COOH. HA–CPN showed much slower phase transition kinetics and a significant increase in GFT. The conjugation of a more hydrophilic component with PNIPAM-COOH increased the GFT because the components hindered the dehydration of the polymer chains and played a part in expanding the collapsed structure. Nonetheless, the GFT was <5 min for polymer solution and the gel could be plated easily.

Similar to GFT, the GLT was also strongly affected by the addition of chitosan and HA components but the value could be increased up to 6 times in comparison to GFT (Fig. 3b). PNIPAM-COOH shows the shortest GLT while CPN and HA–CPN hydrogel exhibited much longer GLT (*ca.* 15 min), implying that gelation of more complicated molecules might lead to more complicated physical entanglement among polymer chains and longer liquefaction time is required for high-molecular weight polymers to rearrange and disentangle inter- and intra-molecular chains. In addition, polymer concentration appeared to play an important role in changing the GLT. Hydrogels formed with a higher polymer concentration showed a retarded response to temperature decrease, leading to resultant increase in GLT (data not shown).

Hydrogels are hydrophilic polymer networks, which may absorb, at an equilibrium swelling level, up to thousands of times their dry weight in water. Hence, the value of water content in a hydrogel can be viewed as an index to determine the efficiency of transport of nutrients into and poisonous waste out of the gel [10]. The water content of hydrogel equilibrated at 37 °C was dependent upon the concentration and composition of the hydrogels (Table 2). Owing to the effect of volume repulsion between polymer molecules and water molecules, more concentrated polymer solution resulted in hydrogels with lower water contents. Owing to the contribution of chitosan and HA components, known for high water sorption and water retention, in the polymer hydrogels, the CPN and HA–CPN hydrogels contain significantly more water than the PNIPAM-COOH hydrogel. This may imply that the adsorption (or partitioning) and diffusion of solutes through the interior tunnels can be more facile in the CPN and HA–CPN hydrogels. At the lowest polymer concentration (5% (w/v)), CPN solution did not form rigid gel at 37 °C but gave white precipitates. Nonetheless, 5% (w/v) HA–CPN gelled successfully at 37 °C and exhibited the highest water content, implying that HA played an important role in stabilizing the integrity of 3D structure of polymer hydrogels.

The volume shrinkage of various hydrogels after gel formation is also compared in Table 2. PNIPAM-COOH hydrogel showed considerable volume shrinkage up to 90% due to its intrinsically thermo-contractive behavior. The addition of chitosan and HA significantly decreased the extent of collapse as in comparison to PNIPAM-COOH. From a tissue engineering perspective, scaffolds featured with enormous volume collapses at physiological temperature may represent several drawbacks, such as squeezing the cells out of the scaffold, damaging the cells, increasing the difficulty of clinical transplantation, and hindering the ability of tissue repair due to a huge gap occurred between the cell/scaffold construct and the native tissue [29]. CPN and HA–CPN hence could significantly improve the volume contraction during gel formation by reducing the extent of structure collapse up to 1/4 of the value associated with PNIPAM-COOH.

The morphology of the various copolymers was examined by WXRD as shown in Fig. 4. The copolymers exhibited two diffraction peaks at 7.5° and 20°, which correspond to the crystalline structure of linear PNIPAM-COOH. The diffractograms also show peaks at 20° and 27° for chitosan and HA, respectively, indicating crystalline structure of those linear polymers (data not shown). Only minor decrease of relative intensity was observed when PNIPAM-COOH was grafted to chitosan, indicating minor interference of the crystalline formation for CPN. However, a substantial decrease in peak intensity was observed when CPN was conjugated to HA and the

Table 2
The water content and volume shrinkage of polymer hydrogels at different polymer concentrations.

Conc.(% (w/v))	Water content (g water/g polymer)			Volume shrinkage (%)		
	PNIPAM-COOH	CPN	HA–CPN	PNIPAM-COOH	CPN	HA–CPN
5	2.60 ± 0.24	NA	14.3 ± 0.1	−87.0 ± 8.0	NA	−19.8 ± 0.1
10	1.25 ± 0.04	7.04 ± 0.02	7.62 ± 0.08	−87.6 ± 2.8	−23.9 ± 0.1	−20.7 ± 0.2
20	0.32 ± 0.01	2.97 ± 0.25	3.12 ± 0.09	−93.7 ± 2.9	−40.7 ± 3.4	−37.6 ± 1.1

Polymer hydrogels were gelled at 37 °C for 2 days. NA represents data not available because of structure collapse and incomplete gelation. Data were reported as mean ± standard deviation ($N = 6$).

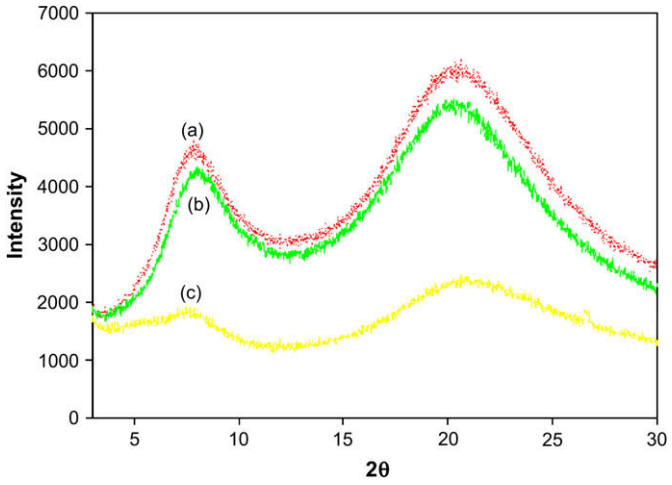

Fig. 4. XRD spectra of (a) PNIPAM-COOH, (b) CPN, and (c) HA–CPN.

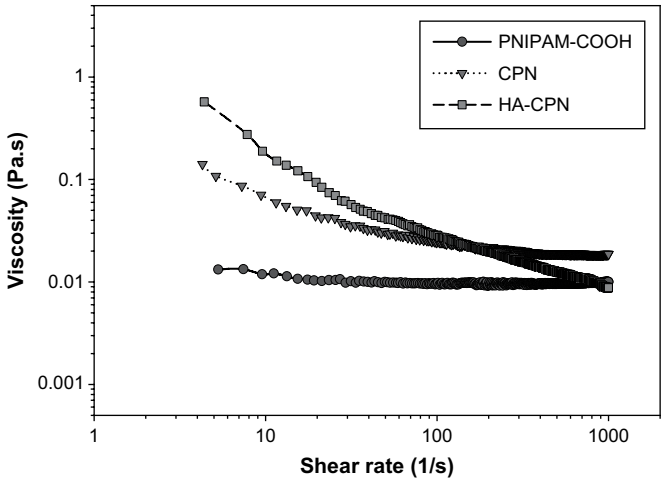

Fig. 6. The effect of shear rate on viscosity of 10% (w/v) polymer solution at 25 °C.

introduction of CPN bulky pendant groups to the linear HA polymer chain, which decreases the crystallinity structure of HA–CPN copolymer substantially.

Since the mechanical property of hydrogel was greatly influenced by the gel-forming polymer component, the complex shear modulus (G^*) of hydrogels was measured at different temperatures as an index of its mechanical strength (Fig. 5a). Within the tested temperature range (28–42 °C) tested, the moduli rose sharply at temperatures close to 31 °C, corresponding to temperature where polymer solution turned into a gel-like structure. Obviously, the introduction of chitosan could significantly improve the mechanical strength of PNIPAM-COOH, however, the G^* value was reduced from 495 Pa for CPN to 210 Pa for HA–CPN at 37 °C. This phenomenon probably may be due to the high-molecular weight of HA, which causes the whole molecular structure to be more flexible and less dense during hydrogel formation. PNIPAM hydrogel is generally associated with insufficient mechanical strength. To solve this limitation, several publications reported the combination of PNIPAM with other natural polymers to improve the mechanical strength [12,30]. The results from G^* measurements indicate that introducing chitosan and HA into PNIPAM not only retains the thermo-responsive characteristics of PNIPAM, but also effectively strengthens the mechanical property of the formed hydrogel. From a tissue engineering perspective, this increase in stiffness represents *in situ* stabilization and a more substantial structure that may better support tissue growth.

The dependence of polymer solution viscosity on temperature is shown in Fig. 5b. At temperatures above phase transition temperature, an abrupt increase in viscosity marks the onset of the gelation process. The gelling temperature increased in the order of PNIPAAM-COOH ≈ CPN (29.1 °C) < HA–CPN (30 °C), which is similar to the LCST determined by the UV method.

Ideal injectable hydrogels should offer low resistance to shear flow, once the plunger starts to move, the viscosity should decrease to allow the hydrogel to be injected with little energy expenditure. Otherwise, at rest, they should possess high equilibrium viscosity to ensure an appropriate maintenance of the defect space. To ascertain the hydrogel resistance to flow through a syringe, polymer solutions were subjected to steady-state flow shear tests at 25 °C. The flow curves with viscosity plotted as a function of the shear rate are reported in Fig. 6. For both CPN and HA–CPN, the viscosity decreased by increasing the shear rate, that is, these systems showed a shear thinning or a pseudoplastic behavior. In contrast, PNIPAM-COOH hydrogel showed a Newtonian behavior with constant but rather low viscosity. The injectable application requires an injection through a syringe in which high shear rates are reached. Both CPN and HA–CPN show a shear thinning or pseudoplastic behavior, that is an appropriate feature for the injectable applications. To further model the flow properties, we used the Cross-equation from which the flow parameters n (pseudoplasticity index), and the zero-shear viscosity (η_o), were determined. The zero-shear viscosity reflects the ability of the

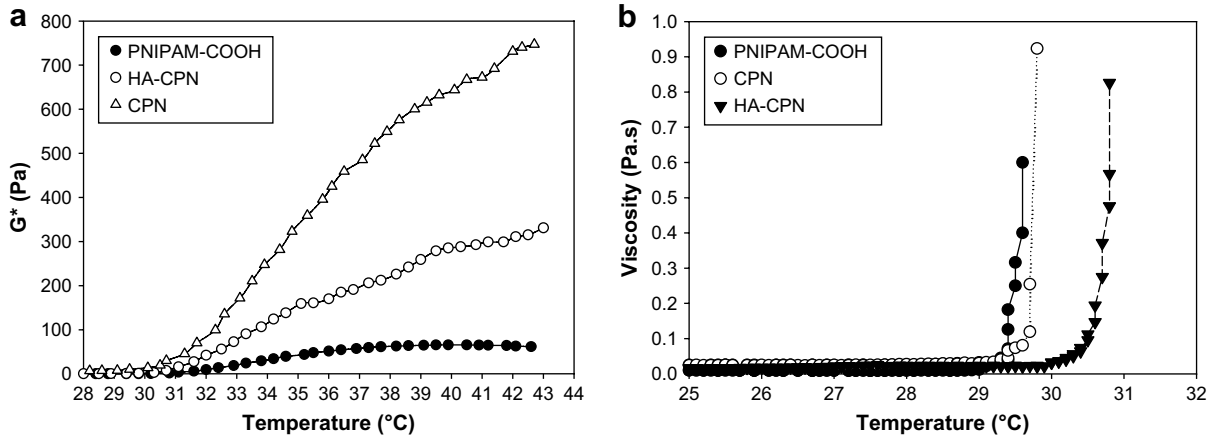

Fig. 5. (a) The complex shear modulus and (b) viscosity of different polymer hydrogels as a function of temperature. The concentration of polymer solution is 10% (w/v).

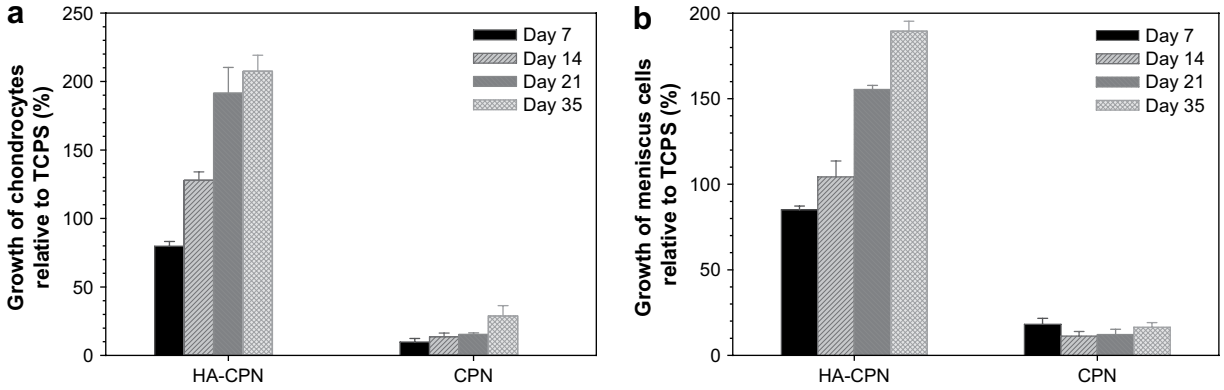

Fig. 7. Proliferation of (a) chondrocytes and (b) meniscus when cultured in hydrogels. Data represent mean ± standard deviation and are expressed as the percentage with respect to TCPS controls. The initial cell density was 1.0×10^5 cells. Polymer concentration was 10% (w/v) for all hydrogel scaffolds.

formulations to maintain the injected spaces at rest or when subjected to a very low shear rate deformation. For CPN, the η_o value (0.26) is much lower than that of HA–CPN (2.77) and highlights that HA–CPN possesses the right requirements to maintain the injected spaces and to provide mechanical support to tissue growth. The parameter n can be utilized to compare the shear thinning properties of the various systems since it represents the slope of the shear rate dependent region of the flow curve and it varies from 0 to 1 when moving from a Newtonian fluid behavior to a more pseudoplastic one. HA–CPN gives a higher value of parameter n (0.53) than that of CPN (0.18), indicating an easy administration of this system.

3.3. Cultivation of chondrocytes and meniscus cells in hydrogels

Proliferation of viable chondrocytes and meniscus cells in hydrogel scaffolds is shown in Fig. 7 where data are normalized with the values obtained from TCPS controls in each experiment and reported as percentage relative to TCPS controls. For HA–CPN, the cell numbers were lower than those of control only during the first week throughout the culture period. However, enhanced cell growth was observed thereafter with the cell number reaching 207% and 189% of those from TCPS for chondrocytes and meniscus cells, respectively, after 5 weeks. It has been reported that cell proliferation rate was reduced initially (during the first week) due to re-differentiation when chondrocytes were seeded into a 3D environment after monolayer culture, which is consistent with current findings [31].

Nonetheless, cell proliferation in HA–CPN was significantly higher than that in CPN. The percentage of growth for both cells was quite small (*ca.* 10–40%) when cells were cultured in CPN. Cell growth inhibition could be attributed to the high positive charges (NH_3^+) associated with chitosan backbone [32,33]. The difference in surface potentials between CPN and HA–CPN in Table 1 provides strong evidence to explain why cells cultured in CPN displayed poor proliferation ability. However, the difference in cell growth could also be due to cells being able to better attach to the HA-containing copolymer or due to diffusion of large molecular weight species to the cells in those gels. In view of the poor proliferation ability for cells cultured in CPN, only HA–CPN was subject to further cell culture study hereafter.

GAG and collagen are two major components of the ECM found in cartilage and meniscus. Hence, the total collagen produced by chondrocytes and meniscus cells can be viewed as an important index to assess the differentiation of cells. As shown in Fig. 8, total collagen and GAG production showed a continuous increase with increasing culture time. Progressive tissue formation, as indicated by the accumulation of ECM, occurred throughout the entire culture period. In accordance with cell proliferation ability, enhanced production of both ECM components was evident after cells were cultured in HA–CPN for 2 weeks when compared to those cultured on TCPS. At the end of culture period, the amount of

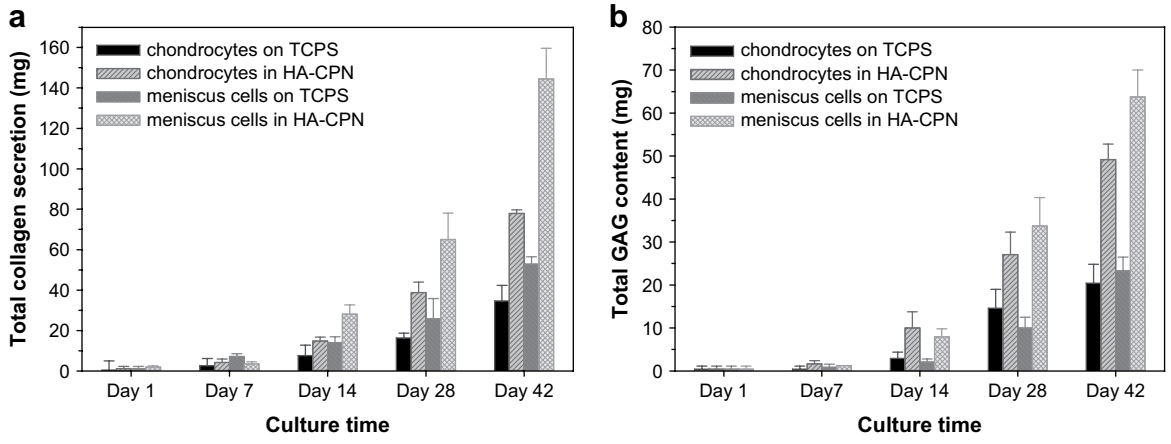

Fig. 8. (a) Total GAG and (b) total collagen synthesized by rabbit articular chondrocytes and meniscus cells in HA–CPN hydrogel and on TCPS. Initial cell seeding density is 2.2×10^5 cells.

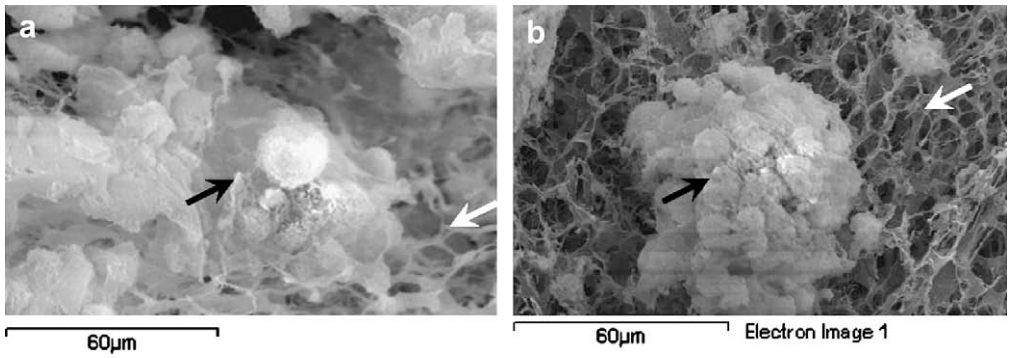

Fig. 9. Scanning electron micrographs of (a) chondrocytes and (b) meniscus cells seeded in HA–CPN hydrogel scaffold after cultured for 42 days. Magnification is ×1000. Bar is 60 μm. Black arrows represent cells, and white arrows stand for the micro-structure of polymer hydrogel scaffold.

GAG and collagen produced by chondrocytes in HA–CPN was 241% and 225% of those produced by cells cultured on TCPS, respectively. During the same period, GAG and collagen production by meniscus cells in HA–CPN were 273% and 272% of those produced by cells cultured on TCPS, respectively. Up-regulating collagen production could provide increased mechanical stability and aid in decreasing GAG loss to the surrounding media [34]. These observations implied that HA–CPN hydrogel scaffold provided a 3D cell arrangement mimicking the *in vivo* situation of native tissues to encourage more ECM deposition than monolayer TCPS culture system.

The SEM images in Fig. 9 show that when chondrocytes and meniscus cells were cultured in HA–CPN for 42 d, the cells were embedded within the secreted matrix, an evidence of cell function for ECM secretion. At the same time, both cells also retained their correct phenotypes. Compared with the *in vitro* expansion of isolated cells showing an elongated morphological appearance in TCPS monolayer culture, chondrocytes and meniscus cells grown in HA–CPN could maintain a spherical morphology with smooth outlines, and a round morphology is known to be one of the characteristics of differentiated chondrocytes [35]. Initial expansion on TCPS will elicit de-differentiation of chondrocytes [36]; however, the de-differentiated chondrocytes could be induced to re-differentiation by culturing the cells in HA–CPN hydrogel, which provides 3D environment to favor a spherical morphology. It has been proven that scaffolds where the cultured chondrocytes remain spherical

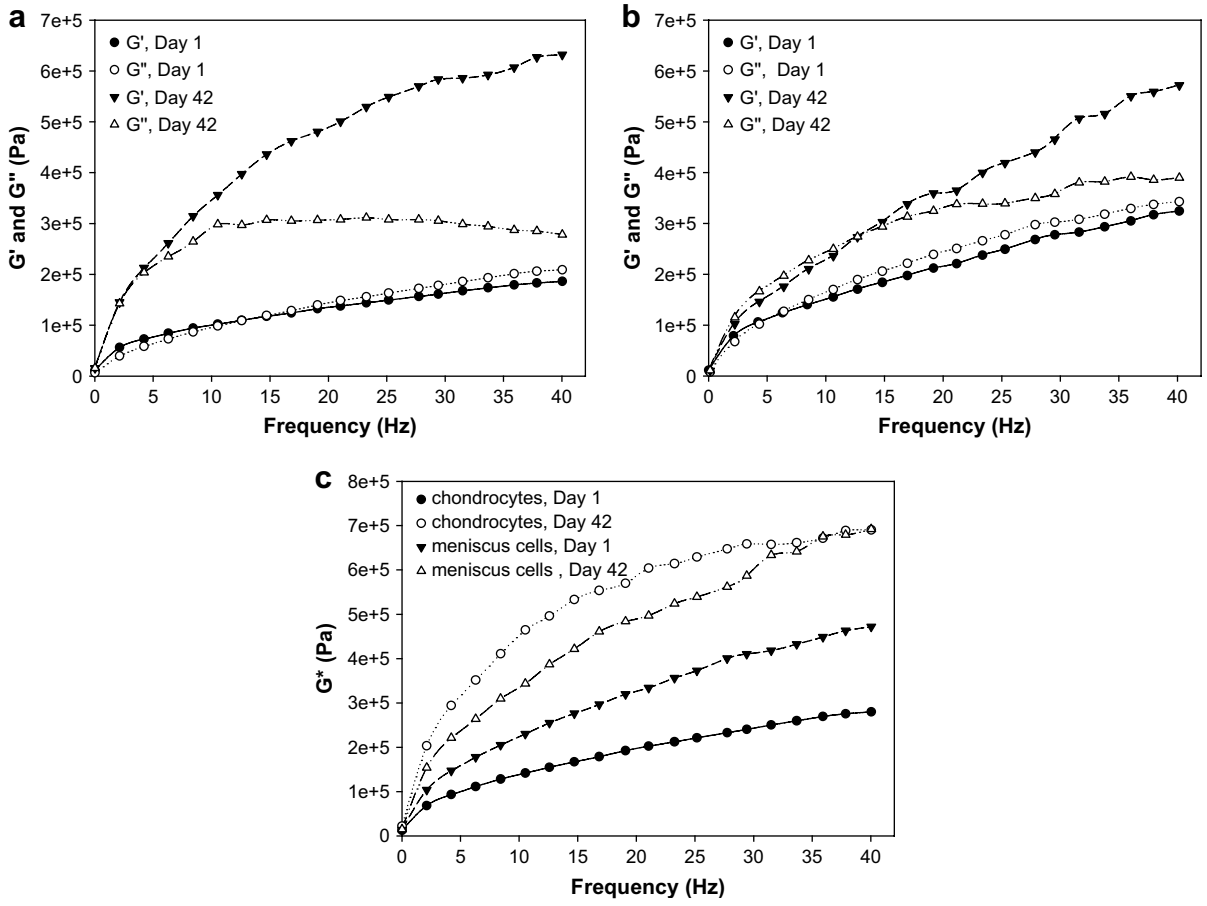

Fig. 10. The storage (G'), loss (G''), and complex (G^*) modulus of cells/HA–CPN hydrogel constructs at 37 °C at different culture times. (a) G' and G'' for chondrocytes. (b) G' and G'' for meniscus cells. (c) G^* for chondrocytes and meniscus cells. The concentration of polymer solution is 10% (w/v). Initial cell density = 2.2×10^5 cells.

and produce ECM components could be potential candidates for cartilage tissue engineering applications [37,38]. From background porous structure shown in Fig. 9, the micrographs also show that 10% (w/v) HA–CPN hydrogel scaffold was with interconnected pores between 5 and 10 μm in diameter.

To evaluate the macroscopic mechanical behavior of cell/hydrogel constructs, the constructs were subject to rheological studies during the start (day 1) and end (day 42) of culture period. The elastic and loss moduli as a function of frequency for the gelled polymer solutions at 37 °C are reported in Fig. 10a and b. All the systems display frequency-dependent moduli and in particular, by increasing the frequency, both moduli increase. The values of G' and G'' also depend on culture time, but the extent of increase is more pronounced for G' than that of G'', indicating that the cell/scaffold construct will show a more viscoelastic behavior with time. Differences among the rheological behaviors of the construct with culture time are observed. For constructs cultured for 1 day, the viscous modulus is higher than the elastic modulus in most of the frequency range, indicating that the construct behaviors as viscous solution. Constructs cultured for 42 days, instead, at low frequency, show a predominant viscous character ($G'' > G'$) but, by increasing the frequency, the elastic modulus grows faster than the viscous one so that G' curve crosses G'' curve at a frequency called cross-over frequency. At frequency higher than cross-over frequency, the elastic modulus prevails on the viscous one and the system shows a predominant elastic character. This rheological behavior is typical of an entangled network and provides evidence of interactions of cell ECM components with copolymer chains in the cell/hydrogel constructs during cell growth [39,40].

G^* value and mechanical strength of the artificial cartilage and meniscus constructs also increased substantially with culture time (Fig. 10c). G^* values increased to 2.47 and 1.47-fold of their initial values at the end of culture period for chondrocytes and meniscus cells, respectively. This could be ascribed to increasing concentration of functional ECM components in the hydrogel with culture time, which are excreted by entrapped chondrocytes and meniscus cells. The compressive complex modulus values could vary from one type of measurement to another, but, in general, they can be used to have an overview of the mechanical range of response of chondrocytes and meniscus tissues. After cultured for 6 weeks in HA–CPN, both constructs gave ultimate G^* values close to 0.7 MPa, which are in-line with the values reported before. The compressive modulus of cartilage tissues from animal sources has been reported to be 0.78–0.81 MPa for porcine neonatal articular cartilage and 0.41–0.79 MPa for bovine knee meniscal tissue [41]. Recently, equilibrium compressive modulus values of 0.06 MPa and 0.13 MPa were reported for native and tissue-engineered bovine menisci, respectively [42]. Judging from the similar mechanical response of cells-loaded hydrogel, HA-CPN could be deemed suitable for cartilage and meniscus tissue regeneration.

4. Conclusions

In this study, thermo-responsive polymer hydrogels consisting of chitosan, HA and PNIPAM were fabricated successfully. Their potential as cartilage and meniscus tissue engineering scaffolds was also evaluated. Our findings demonstrated that CPN and HA–CPN hydrogels have several advantages including reversibly soluble–insoluble characteristics, high water content, excellent resistance to structure collapse, and significant improvement in mechanical strength over PNIPAM-COOH. Although additional grafting of HA to CPN will lead to reduced mechanical strength, it will also provide a polymer solution with better flow property as an injectable cell carrier and alleviate limitation on cell proliferation. Overall, rabbit articular chondrocytes and meniscus cells cultured in HA–CPN hydrogel scaffolds showed beneficial effects on cell phenotypic morphology, proliferation, and differentiation. Progressive tissue formation was demonstrated by monotonic increases in ECM contents and mechanical properties. This study suggested that HA–CPN copolymer hydrogel may be well suited as a carrier material for the transplant of chondrocytes and meniscus cells or as a scaffold for the tissue engineering of cartilage-like and meniscus-like tissues.

Acknowledgements

Financial supports from National Science Council of the Republic of China and Chang Gung Memorial Hospital are highly appreciated.

References

[1] Vinatier C, Magne D, Weiss P, Trojani C, Rochet N, Carle GF, et al. Biomaterials 2005;26:6643–51.
[2] Lee JE, Kim KE, Kwon IC, Ahn HJ, Lee SH, Cho H, et al. Biomaterials 2004; 25:4163–73.
[3] Kumar MNV. React Funct Polym 2000;46:1–27.
[4] Khor E, Lim LY. Biomaterials 2003;24:2339–49.
[5] Van de Vord PJ, Matthew HWT, DeSilva SP, Mayton L, Wu B, Wooley PH. J Biomed Mater Res 2002;59:585–90.
[6] Kakehi K, Kinoshita M, Yasueda SI. J Chromatogr B 2003;797:347–55.
[7] Forsey RW, Fisher J, Thompson J, Stone MH, Bell C, Ingham E. Biomaterials 2006;27:4581–90.
[8] Miralles G, Baudoin R, Dumas D, Baptiste D, Hubert P, Stoltz JF, et al. J Biomed Mater Res 2001;57:268–78.
[9] Hoffman AS. Adv Drug Delivery Rev 2002;43:3–12.
[10] Drury JL, Mooney DJ. Biomaterials 2003;24:4337–51.
[11] Kost J, Langer R. Adv Drug Delivery Rev 2001;46:125–48.
[12] Kim JH, Lee SS, Kim SJ, Lee YM. Polymer 2002;43:7549–58.
[13] Wang LQ, Tu K, Li Y, Zhang J, iang L, Zhang Z. React Funct Polym 2002;53: 19–27.
[14] Morikawa N, Matsuda T. J Biomater Sci Polym Ed 2002;13:167–83.
[15] Ohya S, Nakayama Y, Matsuda T. Artif Organs 2001;4:308–14.
[16] Ohya S, Sonoda H, Nakayama Y, Matsuda T. Biomaterials 2005;26:655–9.
[17] Ohya S, Matsuda T. J Biomater Sci Polym Ed 2005;16:809–27.
[18] Lee SB, Ha DI, Cho SK, Kim SJ, Lee YM. J Appl Polym Sci 2004;92:2612–20.
[19] Chenite A, Chaput C, Wang D, Combes C, Buschmann MD, Hoemann CD, et al. Biomaterials 2000;21:2155–61.
[20] Cho JH, Kim SH, Park KD, Jung MC, Yang WI, Han SW, et al. Biomaterials 2004;25:5743–51.
[21] Lee JW, Jung MC, Park HD, Park KD, Ryu GH. J Biomater Sci Polym Ed 2004;15:1065–79.
[22] Chen JP, Cheng TH. Macromol Biosci 2006;6:1026–39.
[23] Fong JY, Chen JP, Leu YL, Hu JW. Drug Delivery 2008;15:235–43.
[24] Chen JP, Cheng TH. Colloid Surf A 2008;313–314:254–9.
[25] Fong JY, Chen JP, Leu YL, Hu JW. Eur J Pharm Biopharm 2008;68:626–36.
[26] Armstrong DC, Johns MR. Biotechnol Tech 1995;9:491–6.
[27] Cross MMJ. Colloid Interf Sci 1965;20:417–37.
[28] Gil ES, Hudson SM. Prog Polym Sci 2004;29:1173–222.
[29] Loguercio AD, Reis A, Ballester RY. Dent Mater 2004;20:236–43.
[30] Wang M, Fang Y, Hu D. React Funct Polym 2001;48:215–21.
[31] Izquierdo R, Garcia-Giralt N, Rodriguez MT, Caceres E, Garcia SJ, Gomez Ribelles JL, et al. J Biomed Mater Res 2008;85A:25–35.
[32] Suh JKF, Mattew HWT. Biomaterials 2000;21:2589–98.
[33] Tan W, Krishnaraj R, Desai TA. Tissue Eng 2001;7:203–12.
[34] Neves AA, Medcalf N, Brindle KM. Biomaterials 2005;26:4828–36.
[35] Li A, Zhang M. J Biomed Mater Res 2005;75A:485–93.
[36] von der Mark K, Gauss V, von der Mark H, Muller P. Nature 1977;267:531–2.
[37] Russlies M, Behrens P, Wunsch L, Gille J, Ehlers EM. Ann Anat 2002;184: 317–23.
[38] Hsu SH, Whu SW, Hsieh SC, Tsai CL, Chen DC, Tan TS. Artif Organs 2004;28: 693–703.
[39] Ambrosio L, Borzacchiello A, Netti PA, Nicolais L. J Macromol Sci A 1999; A36:991–1000.
[40] Maltesea A, Borzacchiellob A, Mayolc L, Bucoloa C, Maugeria C, Nicolaisb L, et al. Biomaterials 2006;27:5134–42.
[41] Almarza AJ, Athanasiou KA. Ann Biomed Eng 2004;32:2–17.
[42] Ballyns JJ, Gleghorn JP, Niebrzydowski V, Rawlinson JJ, Potter HG, Maher SA, et al. Tissue Eng 2008;14:1195–202.